Human Molecular Genetics, 2010, Vol. 19, No. 17 **3332–3342**
doi:10.1093/hmg/ddq237
Advance Access published on June 10, 2010

Reduced expression of Pax6 in lens and cornea of mutant mice leads to failure of chamber angle development and juvenile glaucoma

Markus Kroeber[1], Noa Davis[2], Silvia Holzmann[1], Michaela Kritzenberger[1], Michal Shelah-Goraly[3], Ron Ofri[3], Ruth Ashery-Padan[2] and Ernst R. Tamm[1,*]

[1]Institute of Human Anatomy and Embryology, University of Regensburg, Regensburg, Germany, [2]Sackler Faculty of Medicine, Tel Aviv University, Tel Aviv, Israel and [3]Koret School of Veterinary Medicine, Hebrew University of Jerusalem, Rehovot, Israel

Received May 28, 2010; Revised May 28, 2010; Accepted June 7, 2010

Heterozygous mutations in *PAX6* are causative for *aniridia*, a condition that is frequently associated with juvenile glaucoma. Defects in morphogenesis of the iridocorneal angle, such as lack of trabecular meshwork differentiation, absence of Schlemm's canal and blockage of the angle by iris tissue, have been described as likely causes for glaucoma, and comparable defects have been observed in heterozygous *Pax6*-deficient mice. Here, we employed Cre/loxP-mediated inactivation of a single *Pax6* allele in either the lens/cornea or the distal optic cup to dissect in which tissues both alleles of *Pax6* need to be expressed to control the development of the tissues in the iridocorneal angle. Somatic inactivation of one allele of *Pax6* exclusively from epithelial cells of lens and cornea resulted in the disruption of trabecular meshwork and Schlemm's canal development as well as in an adhesion between iris periphery and cornea in juvenile eyes, which resulted in the complete closure of the iridocorneal angle in the adult eye. Structural changes in the iridocorneal angle presumably caused a continuous increase in intraocular pressure leading to degenerative changes in optic nerve axons and to glaucoma. In contrast, the inactivation of a single *Pax6* allele in the distal optic cup did not cause obvious changes in iridocorneal angle formation. We conclude that the defects in iridocorneal angle formation are caused by non-autonomous mechanisms due to *Pax6* haploinsufficiency in lens or corneal epithelial cells. Pax6 probably controls the expression of signaling molecules in lens cells that regulate the morphogenetic processes during iridocorneal angle formation.

INTRODUCTION

PAX6, a transcription factor that has been highly conserved during evolution, is a key regulator of eye development in both vertebrates and invertebrates (1–4). In humans, heterozygous mutations in *PAX6* are causative for *aniridia*, a condition associated with a variety of ocular developmental anomalies including deficiency or hypoplasia of the iris, corneal opacities, foveal and optic nerve dysplasia and cataract (5–7). More rarely, mutations in *PAX6* lead to Peters' anomaly (8), a condition that is characterized by a central corneal opacity (leukoma), a local absence of the corneal endothelium (to which the lens may adhere to) and iridocorneal adhesions (9). In mice with heterozygous mutations in *Pax6*, ocular defects are in general more extreme. In most cases, the eyes are less than half of their normal size (microphthalmos), the anterior chamber of the eye is missing, the retina is abnormally folded and the lens is absent or small and has anterior cataracts (10–13). About 50–75% of patients with *aniridia* develop an increase in intraocular pressure (IOP) in preadolescent or early adult years that commonly leads to optic nerve damage and glaucoma (5–7). IOP is generated via the aqueous humor circulation system (14). Aqueous humor is secreted by the ciliary processes into the posterior chamber of the eye and leaves the eye through the trabecular meshwork and Schlemm's canal, which are both localized at the iridocorneal angle of the

*To whom correspondence should be addressed at: Institute of Human Anatomy and Embryology, University of Regensburg, Universitätsstr. 31, 93053 Regensburg, Germany. Tel: +49 9419432839; Fax: +49 9419432840; Email: ernst.tamm@vkl.uni-regensburg.de

anterior chamber (15). Studies in heterozygote Pax6-deficient mice, an animal model of *aniridia*, have identified defects in trabecular meshwork differentiation and the complete absence of Schlemm's canal (16). Similar structural defects may well account for the increase in IOP and the glaucoma phenotype, which are observed in humans with *aniridia*.

During the development of the mammalian eye, Pax6 is strongly expressed in those cells that derive from the surface ectoderm or the optic cup (17–20). Both tissues do not directly contribute to the development of the trabecular meshwork and Schlemm's canal. The trabecular meshwork takes its origin from cranial neural crest cells that migrate to the eye, whereas Schlemm's canal derives from blood vessels that penetrate the eye at the cornea–scleral junction (9,21). Some researchers demonstrated a weak immunostaining for Pax6 in neural crest-derived cells during the development of the iridocorneal angle (16,22), a finding that was not confirmed by others (23). At present it is not clear, if the changes in morphogenesis of the iridocorneal angle, which were observed in the eyes of heterozygous Pax6-deficient mice, are caused by cell autonomous or non-autonomous mechanisms.

In order to have a tool that allows dissection of the tissue-specific sensitivity to Pax6 haploinsufficiency, we previously employed the Cre/loxP approach to selectively inactivate a single Pax6 allele in either the developing lens and cornea or the distal optic cup (24). Inactivation in lens/cornea resulted in the formation of a smaller lens and eye, whereas iris development was largely unaffected. In contrast, the dosage of Pax6 in the distal optic cup was essential for the development of the iris, but not relevant for that of the lens. In the present study, we used essentially the same system to dissect in which cell types both alleles of *Pax6* need to be expressed to control the development of the tissues in the iridocorneal angle. We show that the specific deletion of one Pax6 copy from the lens and cornea leads to structural changes during trabecular meshwork and Schlemm's canal development, which are very similar to those that are observed in heterozygous Pax6-deficient mice. In contrast, the specific deletion of Pax6 in the distal optic cup does not lead to obvious developmental changes in the trabecular meshwork or Schlemm's canal. Overall, our findings strongly indicate that the expression of Pax6 in the lens/cornea during embryonic life controls essential signaling processes that are critically required for the generation and the differentiation of the tissues in the iridocorneal angle. Moreover, we demonstrate that failure in the development of the trabecular meshwork and Schlemm's canal following the exclusive inactivation of a single Pax6 allele in the surface ectoderm derivatives leads to an increase in IOP, to optic nerve damage and to glaucoma.

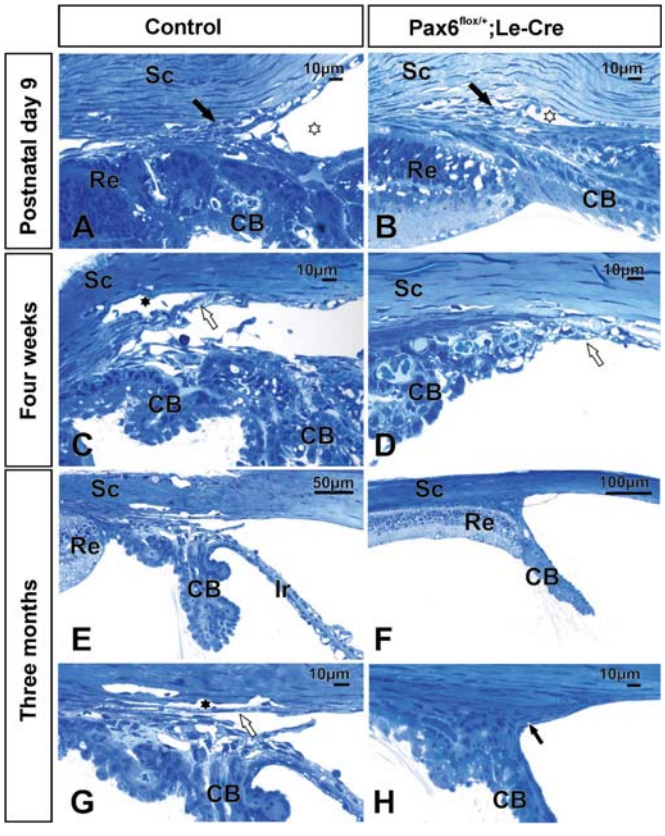

Figure 1. The development of the iridocorneal angle is impaired in the eyes of *Pax6$^{flox/+}$;Le-Cre* mice. Light micrographs of semithin sections from control (*Pax6$^{flox/+}$*) animals (**A**, **C**, **E** and **G**) and *Pax6$^{flox/+}$;Le-Cre* littermates (**B**, **D**, **F** and **H**) at postnatal (P) day 9 (A and B), at 4 weeks (C and D) and 3 months (E–H) of age. (A and B) At P9, both *Pax6$^{flox/+}$;Le-Cre* and control mice show mesenchymal cells (black arrows) and adjacent scleral vessels in their iridocorneal angles. The size of the angle (stars) is considerably more narrow in the *Pax6$^{flox/+}$;Le-Cre* mouse. At the fourth postnatal week, trabecular meshwork (white arrow in C) and Schlemm's canal (star in C) are fully developed in the control animal (C), but essentially absent in the experimental littermates (D). In addition, the root of the iris has become attached to the cornea causing a complete closure of the iridocorneal angle in the *Pax6$^{flox/+}$;Le-Cre* mouse (white arrow D). (E–H) At 3 months of age, the iris root of a *Pax6$^{flox/+}$;Le-Cre* mouse forms a dense layer of epithelial cells (black arrow in H), which attaches to and completely covers the periphery of the cornea (F and H, H is a higher magnification of a section adjacent to F), whereas the iridocorneal angle is wide open in the control littermate (E and G, G is a higher magnification of E). The structure of trabecular meshwork (white arrow in G) and Schlemm's canal (star in G) are essentially normal in the control animal. Re, Retina; CB, ciliary body; Sc, sclera; Ir, iris.

RESULTS

Anterior chamber development is impaired in the eyes of *Pax6$^{flox/+}$;Le-Cre* mice

Differentiation of the iridocorneal angle in the anterior chamber of the mouse eye occurs during the first 2 weeks of postnatal life (9). Initially, the angle is filled by a dense mass of mesenchymal cells, which start to separate from each other at the beginning of the second postnatal week. During this period, vessels appear in the adjacent sclera. These processes were not obviously different between the eyes of *Pax6$^{flox/+}$;Le-Cre* (experimental) mice and their *Pax6$^{flox/+}$* (control) littermates, which both showed mesenchymal cells and adjacent scleral vessels in their iridocorneal angles at postnatal day (P) 9 (Fig. 1A and B). Markedly different between experimental and control animals was the size of the angle, which was considerably more narrow in the eyes of *Pax6$^{flox/+}$;Le-Cre* mice (Fig. 1A and B). During the second postnatal week, mesenchymal cells and vessels in the iridocorneal angle differentiate to form the trabecular meshwork and Schlemm's canal, and the morphogenesis of both structures is complete by the end of the third postnatal week (9). Differentiation of trabecular meshwork and

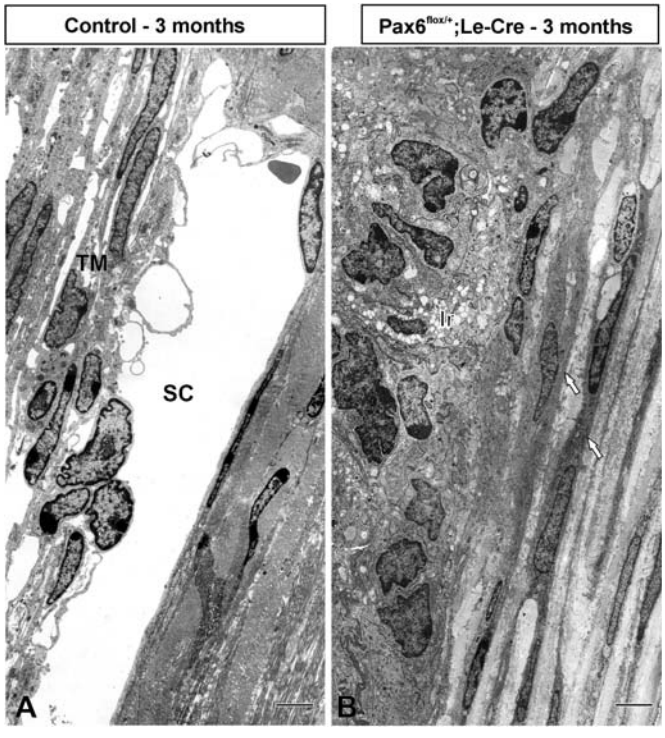

Figure 2. Trabecular meshwork and Schlemm's canal are absent in 3-month-old *Pax6$^{flox/+}$;Le-Cre* mice. Electron micrographs of trabecular meshwork (TM) and Schlemm's canal (SC) in a control animal (**A**) and of the corresponding region in a *Pax6$^{flox/+}$;Le-Cre* mouse (**B**). (A) In the control eye, the lamellae of the TM and SC show an essentially normal structure. (B) In the region that corresponds to the site where TM and SC are localized in control littermates, spindle-shaped cells (arrows) that are embedded in a dense extracellular matrix are observed in experimental mice. The spindle-shaped cells are in direct contact with the epithelial cells of the iris (Ir), whereas the extracellular fibers that surround the cells are continuous with those of sclera and cornea.

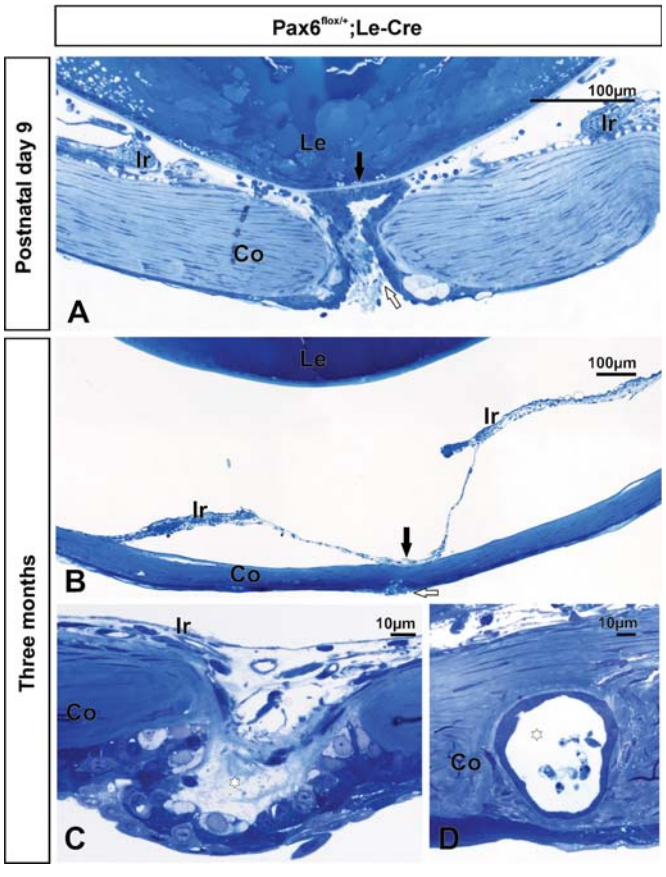

Figure 3. Peters' anomaly in *Pax6$^{flox/+}$;Le-Cre* mice. (**A**) At P9, the lens (Le) is attached to the cornea (Co), and a defect is present in the central corneal stroma (open arrow) through which the corneal epithelium extends to come into contact with the anterior lens capsule (solid arrow). The corneal endothelium is missing in this area. (**B**) At 3 months of age, the lens (Le) is separated from the cornea (Co). In the center of the cornea, the anterior tip of the iris (Ir) is attached to the inner side of the cornea (solid arrow) and the corneal endothelium is missing in this area. At the opposite side of the cornea, there is a small defect in the corneal stroma that is filled with epithelial cells (open arrow). (**C**) Three-month-old *Pax6$^{flox/+}$;Le-Cre* mouse in which iris tissue and lose extracellular matrix (asterisk) fill a central defect in the corneal stroma. (**D**) Three-month-old *Pax6$^{flox/+}$;Le-Cre* mouse with a vesicle (asterisk) in the middle of the central corneal stroma, which is surrounded by epithelial cells that show the structural characteristics of corneal epithelial cells.

Schlemm's canal did not occur in the eyes of *Pax6$^{flox/+}$;Le-Cre* mice; and at the fourth postnatal week, both structures were only present in the eyes of *Pax6$^{flox/+}$* or *Pax6$^{+/+}$* littermates (Fig. 1C), or *Le-Cre* mice, but were essentially absent in experimental littermates (Fig. 1D). Notably, the root of the iris had become attached to the cornea causing a complete closure of the iridocorneal angle in *Pax6$^{flox/+}$;Le-Cre* mice (Fig. 1D). At 3 months of age, the iris root of *Pax6$^{flox/+}$;Le-Cre* mice formed a dense layer of epithelial cells, which attached to and completely covered the periphery of the cornea (Fig. 1F and H), whereas the iridocorneal angle was wide open in the control littermates (Fig. 1E and G). In the region that corresponded to the site where trabecular meshwork and Schlemm's canal was localized in control littermates (Fig. 2A), spindle-shaped cells that were embedded in a dense extracellular matrix were observed in experimental mice by electron microscopy (Fig. 2B). The spindle-shaped cells were in direct contact with the epithelial cells of the iris, whereas the extracellular fibers that surrounded the spindle-shaped cells were continuous with those of sclera and cornea. The electron microscopical analysis supported the results of the histological analysis confirming the complete absence of the trabecular meshwork and Schlemm's canal in the eyes of *Pax6$^{flox/+}$;Le-Cre* experimental mice.

Structural abnormalities in the eyes of *Pax6$^{flox/+}$;Le-Cre* mice were not confined to the periphery of the anterior chamber, but were also observed in its center. In newborn mice, the lens had not become separated from the lens stalk during early eye development and remained attached to the cornea throughout the first postnatal days. Consequently, a defect was present in the central corneal stroma, through which the corneal epithelium extended to come into contact with the anterior lens capsule (Fig. 3A). The corneal endothelium was missing in this area. Beyond the third postnatal week, the lens had usually become separated from the cornea (Fig. 3B). In the center of the cornea, where the lens stalk had persisted and the corneal endothelium had not been formed, the anterior tip of the iris remained attached to the inner side of the cornea (Fig. 3B). Upon higher magnification, iris tissue and lose extracellular matrix were seen to

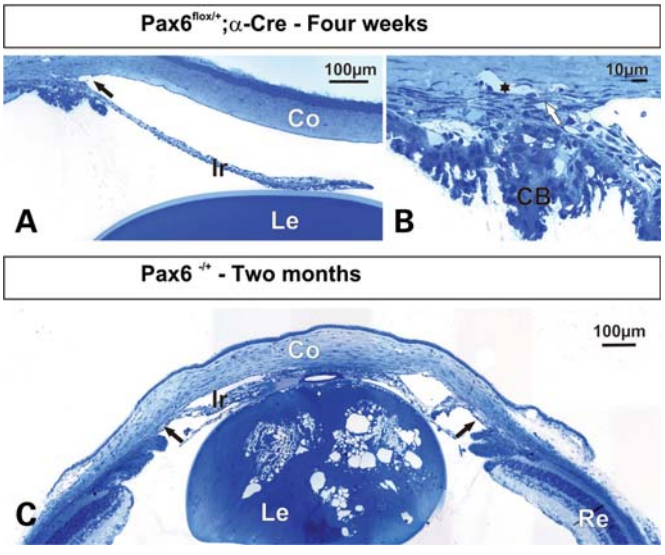

Figure 4. The development of the iridocorneal angle is normal in *Pax6*$^{flox/+}$*;α-Cre* mice, but severely modified in *Pax*$^{-/+}$ mice. (**A** and **B**) Light micrographs of semithin sections from a *Pax6*$^{flox/+}$*;α-Cre* mouse at 4 weeks of age. The iridocorneal angle is wide open (black arrow, A). At higher magnification (B), a normal structured trabecular meshwork (white arrow) and Schlemm's canal (star) can be observed. (**C**) Light micrograph of a semithin section from a *Pax*$^{-/+}$ mouse at 2 months of age. The iris root completely covers the peripheral cornea thereby occluding the iridocorneal angle (arrows). Iridocorneal adhesions are also formed in the region of the pupil, and the lens which contains large vacuoles is attached to the cornea. An anterior chamber is largely absent. Co, Cornea; CB, ciliary body; Le, lens; Ir, iris; Re, retina.

fill the central defect in the corneal stroma through which the lens stalk had persisted in early postnatal life (Fig. 3C). In some of the eyes, a vesicle was seen in the middle of the central corneal stroma, which was surrounded by epithelial cells that showed structural characteristics of corneal epithelial cells and probably took their origin from cells of the persisting lens stalk (Fig. 3D).

Eyes of 3–4-week-old Pax6$^{flox/+}$;α-Cre mice, which were investigated in parallel experiments showed an open iridocorneal angle (Fig. 4A) and no obvious defects in the structure of trabecular meshwork and Schlemm's canal (Fig. 4B). In contrast, the stroma of the iris was markedly thinner when compared with control littermates corroborating previous findings (24). In a previous work, we had observed lack of trabecular meshwork and Schlemm's canal development in 2-week-old *Pax6*$^{-/+}$ mice (16). We now investigated the eyes of 2-month-old *Pax6*$^{-/+}$ animals and found that the iris root completely covered the peripheral cornea to occlude the iridocorneal angle, a structural defect which was quite similar to that seen in the eyes of *Pax6*$^{flox/+}$*;Le-Cre* mice (Fig. 4C). Iridocorneal adhesions were also present in the region of the pupil, and the lens was attached to the cornea. Accordingly, an anterior chamber was largely absent.

IOP is elevated in the eyes of *Pax6*$^{flox/+}$*;Le-Cre* mice

Since the conventional outflow pathways of the aqueous humor, trabecular meshwork and Schlemm's canal, do not form in *Pax6*$^{flox/+}$*;Le-Cre* mice, and the chamber angle

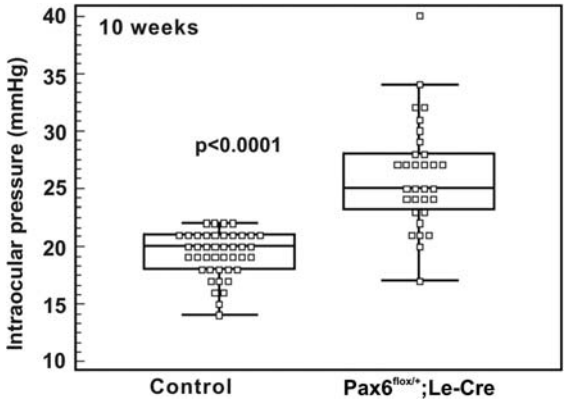

Figure 5. *Pax6*$^{flox/+}$*;Le-Cre* mice show an increase in IOP at 10 weeks of age. IOP was measured invasively in the eyes of 72 animals (41 control and 31 experimental littermates). The box and whisker blot shows median, upper and lower quartile and smallest and greatest values in the distribution. Small squares superimposed on the plot represent individual data points.

becomes blocked by the root of the iris, we were interested to find out if the structural impediment of aqueous humor outflow would lead to an increase in IOP. To this end, we measured IOP invasively by anterior chamber cannulation. As both the root and the anterior tip of the iris were attached to the cornea in experimental mice, the cannula was inserted through the midperiphery of the cornea, where a small anterior chamber was present. IOP was measured in the eyes of 72 animals (41 control and 31 experimental littermates) that were 10 weeks of age. In both control and experimental mice, IOP showed a normal distribution (Fig. 5) and was significantly higher ($P < 0.0001$) in the eyes of experimental mice (26.13 ± 4.62, mean $\pm$ SD) when compared with control animals (19.33 ± 1.94; Fig. 5). To further study the change in IOP over time in *Pax6*$^{flox/+}$*;Le-Cre* mice, we measured IOP non-invasively by tonometry in the eyes of 3–5.5-month-old mice. In marked correlation with the data obtained by invasive measurements, IOP was significantly elevated in Pax6$^{flox/+}$;Le-Cre mice when compared with control animals between 3 and 5.5 months of age (Fig. 6). Because of the large structural abnormalities in the anterior eye of *Pax6*$^{-/+}$ mice, IOP measurements were not performed in this mouse strain.

Optic nerves of *Pax6*$^{flox/+}$*;Le-Cre* mice show axonal damage

In order to learn if the continuous exposure to elevated IOP for several months is causing glaucomatous damage of optic nerve axons, we investigated the optic nerves of 6-month-old *Pax6*$^{flox/+}$*;Le-Cre* mice by light and electron microscopy and compared it with those of their control littermates. In the optic nerve semithin sections from *Pax6*$^{flox/+}$*;Le-Cre* mice, in which myelin sheaths had been stained with 1,4-*p*-phenylenediamine (PPD), multiple dark spots were readily observed that were extremely rare in the optic nerves of control animals (Fig. 7A and B). Subsequent electron microscopy of the dark spots visualized degenerating axons that formed dense and irregular whorls of myelin (Fig. 7C

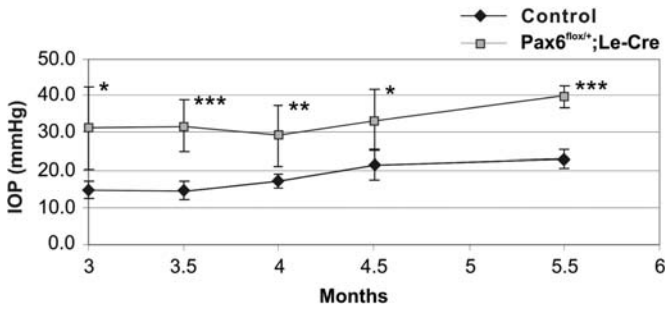

Figure 6. IOP is continuously elevated in the eyes of *Pax6$^{flox/+}$;Le-Cre* mice. IOP was measured non-invasively in control mice and experimental littermates between 3 and 5.5 months of age. Values are mean ± standard deviation of measurements in 10 eyes per genotype at each time point. Two-way ANOVA was performed for statistical analysis, $^{*}P < 0.05$, $^{**}P < 0.01$ and $^{***}P < 0.001$.

and D). In addition, axons were arranged less densely in the optic nerves of *Pax6$^{flox/+}$;Le-Cre* mice when compared with control animals (Fig. 8A and B). In contrast, light and electron microscopy of optic nerves of 4-week-old *Pax6$^{flox/+}$;Le-Cre* mice and control littermates did not show any evidence of degenerating optic nerve axons (Fig. 9C). As a next step, we wanted to support our qualitative observations by obtaining quantitative data. Since lenses and eyes of *Pax6$^{flox/+}$;Le-Cre* mice are smaller than that of control littermates (24), we first wanted to know if the size of the optic nerve is smaller in a small eye, independently of any glaucomatous damage. Indeed, the morphometric analysis of the area covered by optic nerves in a cross section showed that the nerves thicken with increasing age both in *Pax6$^{flox/+}$;Le-Cre* mice and control littermates, but that the area of *Pax6$^{flox/+}$;Le-Cre* optic nerves is ~30–35% smaller than that of controls, irrespective of age (Fig. 9A). We next tested if a smaller size nerve does also contain a smaller number of axons. We therefore counted all axons of the optic nerve in electron micrographs (Fig. 9C) of cross-sectioned nerves from 4-week-old *Pax6$^{flox/+}$;Le-Cre* mice and control littermates. We choose 4 weeks of age, as mouse optic nerve axons are already myelinated at this age, and we had not observed degenerating optic nerve axons at this stage neither in *Pax6$^{flox/+}$;Le-Cre* nor in control animals. Although 49 354 ± 1440 axons were counted in the optic nerves of control animals, only 25 961 ± 5476 were identified in those of *Pax6$^{flox/+}$;Le-Cre* mice (Fig. 9B). We concluded that, compared with control animals, *Pax6$^{flox/+}$;Le-Cre* mice are born with smaller optic nerves containing fewer axons and that absolute measurements would not be appropriate to identify glaucomatous optic nerve damage in *Pax6$^{flox/+}$;Le-Cre* experimental mice. Alternatively, we rather decided to assess the ratio between the total number of degenerating axons as identified in paraphenylenediamine semithin sections (Fig. 8B) and that of the total number of axons. The results clearly showed that there are significantly ($P < 0.05$) more degenerating axons per number of total axons in the optic nerves of experimental mice at 6 months of age (Fig. 10) when compared with control littermates, and strongly supported the assumption that the increase in IOP leads to glaucomatous optic nerve damage in *Pax6$^{flox/+}$;Le-Cre* animals.

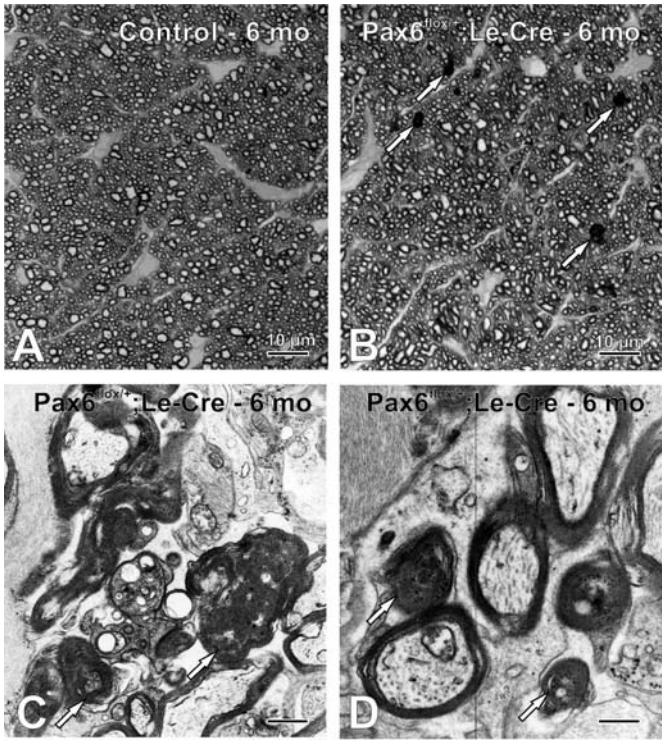

Figure 7. Multiple degenerating axons are present in the optic nerves of 6-month-old *Pax6$^{flox/+}$;Le-Cre* mice. (**A** and **B**) Cross sections of optic nerves from control and *Pax6$^{flox/+}$;Le-Cre* mice stained with paraphenylenediamine. Multiple dark spots (white arrows) are present in the optic nerve of the *Pax6$^{flox/+}$;Le-Cre* mouse. (**C** and **D**) Electron micrographs from the same area as in B. The dark spots that had been visualized by paraphenylenediamine staining represent degenerating axons that form dense and irregular whorls of myelin (arrows).

DISCUSSION

We conclude that the expression of Pax6 in the developing lens and/or cornea plays a critical role for the formation of the aqueous humor drainage structures in the iridocorneal angle of the eye. Somatic inactivation of one allele of *Pax6* exclusively from the epithelial cells of lens and cornea results in the complete disruption of trabecular meshwork and Schlemm's canal development as well as in a growing adhesion between iris periphery and cornea in juvenile eyes, which results in a complete closure of the iridocorneal angle in the adult eye. The structural changes in the iridocorneal angle cause a continuous increase in IOP that finally leads to degenerative changes in optic nerve axons and to glaucoma.

The role of *Pax6* haploinsufficieny in iridocorneal chamber development is non-cell autonomous

The transcription of Pax6 is regulated by multiple transcriptional control elements (25–28). A genomic region which contains the ectoderm enhancer of the *Pax6* promoter drives the expression of Cre in *Le-Cre* transgenic mice (29). The recombination pattern mediated by the *Le-Cre* transgenic line has been characterized in previous studies and includes the cells of the lens, the epithelial layer of the cornea and some amacrine cells in the inner nuclear layer of the retina (24).

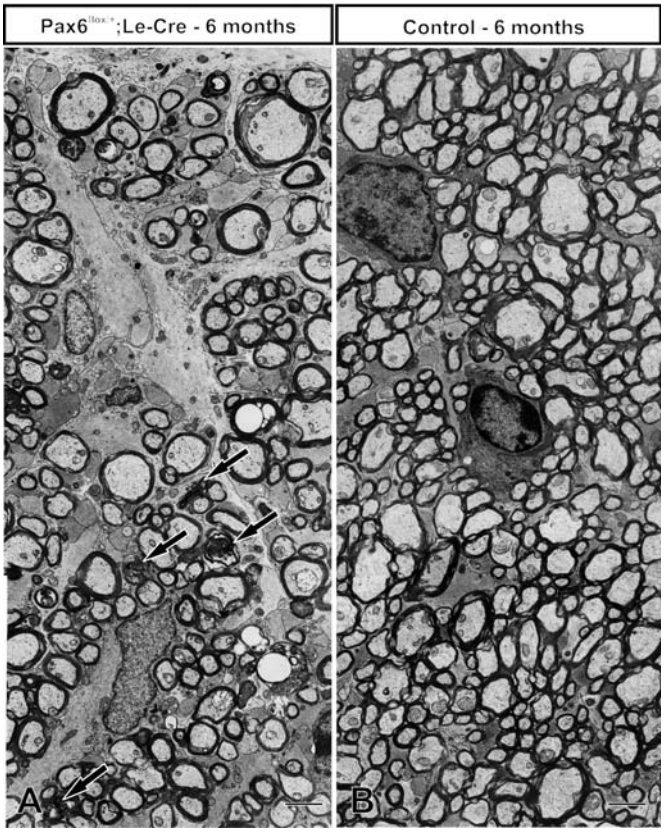

Figure 8. Electron micrographs of optic nerve cross sections from 6-month-old *Pax6$^{flox/+}$;Le-Cre* (**A**) and control (**B**) mice. Axons are arranged less densely in the optic nerve of the *Pax6$^{flox/+}$;Le-Cre* mouse, and multiple degenerating axons are visible (arrows).

Schlemm's canal is a modified blood vessel (30) that derives from the mesoderm, whereas the trabecular meshwork takes its origin from mesenchymal cells of the cranial neural crest (9,23). Since essentially no *Cre*-mediated recombination has been observed in cells of neural crest or mesodermal origin, we conclude that the defects in iridocorneal angle formation in *Pax6$^{flox/+}$;Le-Cre* are caused not by cell autonomous effects but rather by non-autonomous mechanisms due to Pax6 haploinsufficiency in cells outside the iridocorneal angle. The corneal epithelium that covers the outer surface of the cornea and the amacrine cells of the retina are localized distant to the tissues of the iridocorneal angle, and it appears to be unlikely that signaling factors derived from both cell types would have a significant influence on the development of the iridocorneal angle. In contrast, signaling factors secreted from the lens epithelium into the aqueous humor would easily reach the tissues of the iridocorneal angle. It, therefore, seems more likely that the expression of both Pax6 alleles in the lens is required for the formation of the trabecular meshwork and Schlemm's canal, and the morphogenesis of the iridocorneal angle. In α-Cre mice, the Pax6 distal retina enhancer drives the expression of Cre (31), which leads to the specific deletion of one allele of *Pax6* in the distal optic cup in Pax6$^{flox/+}$;α-Cre animals and the formation of a hyoplastic iris (24). Our data show that haploinsufficiency for Pax6 in the distal optic cup does not affect the formation of the trabecular meshwork and Schlemm's canal and indicate that the distal optic cup and the tissues derived from it, iris and ciliary body, play only a minor role for control of iridocorneal angle morphogenesis.

High IOP and glaucoma in *Pax6$^{flox/+}$;Le-Cre* mice

Trabecular meshwork and Schlemm's canal form the trabecular meshwork outflow pathways of the aqueous humor (15). Aqueous humor is actively secreted into the posterior chamber by cells of the ciliary epithelium and flows through the pupil into the anterior chamber (32). When aqueous humor has passed through the trabecular meshwork outflow pathways, it drains into the episcleral venous system outside the eye. The trabecular meshwork outflow pathways are critical in providing resistance to aqueous humor outflow (14,33). IOP builds up in response to this resistance until it is high enough to allow the flow of aqueous humor across the trabecular meshwork into Schlemm's canal. It is not surprising that the structural defects in the trabecular meshwork outflow pathways and the closure of the iridocorneal angle in *Pax6$^{flox/+}$;Le-Cre* mice result in a highly significant and substantial (∼25%) increase in IOP. Still, the increase appears to be moderate when compared with that in human patients following acute closure of the iridocorneal angle, a scenario in which IOP may rise by more than 100%. Compensatory mechanisms very likely prevent a higher increase in IOP in *Pax6$^{flox/+}$;Le-Cre* mice. Such mechanisms may involve the uveoscleral or unconventional outflow route which is open to aqueous humor at the iridocorneal angle in the region of the anterior insertion of iris/ciliary body (34), since there is no complete endothelial or epithelial layer that covers the anterior surface of iris/ciliary body in the mouse eye (35). According to data by Aihara *et al.* (36), almost 80% of the aqueous humor leaves the normal mouse eye via the uveoscleral route, indicating that uveoscleral outflow is substantially higher in the mouse eye as in other mammalian species investigated such as humans, monkeys and rabbits (34).

In several prospective, randomized, multicenter clinical studies, IOP has been identified as the most critical risk factor for the development of glaucoma and axonal damage at the optic nerve head (37–42). Similarly, an increase in IOP does also lead to glaucomatous optic nerve damage in several genetically modified mouse strains (43–46). Glaucomatous damage in mouse and man is characterized by the loss of optic nerve axons and retinal ganglion cells, a parameter that was difficult to evaluate in *Pax6$^{flox/+}$;Le-Cre* mice. The specific deletion of one allele of *Pax6* in lens and cornea results in the formation of eyes which are smaller than that of control animals and which have smaller optic nerves with fewer axons even in young animals, in which glaucomatous damage has not yet occurred. Comparable findings have been reported for the eyes of male heterozygous Sey/+ mice with mutated Pax6 (47). At 6 months of age, optic nerves of *Pax6$^{flox/+}$;Le-Cre* mice contain numerous degenerating axons with structural characteristics similar to those described in other mouse models of glaucoma (48). On a relative scale, the number of degenerating axons is significantly higher than in control eyes, strongly indicating

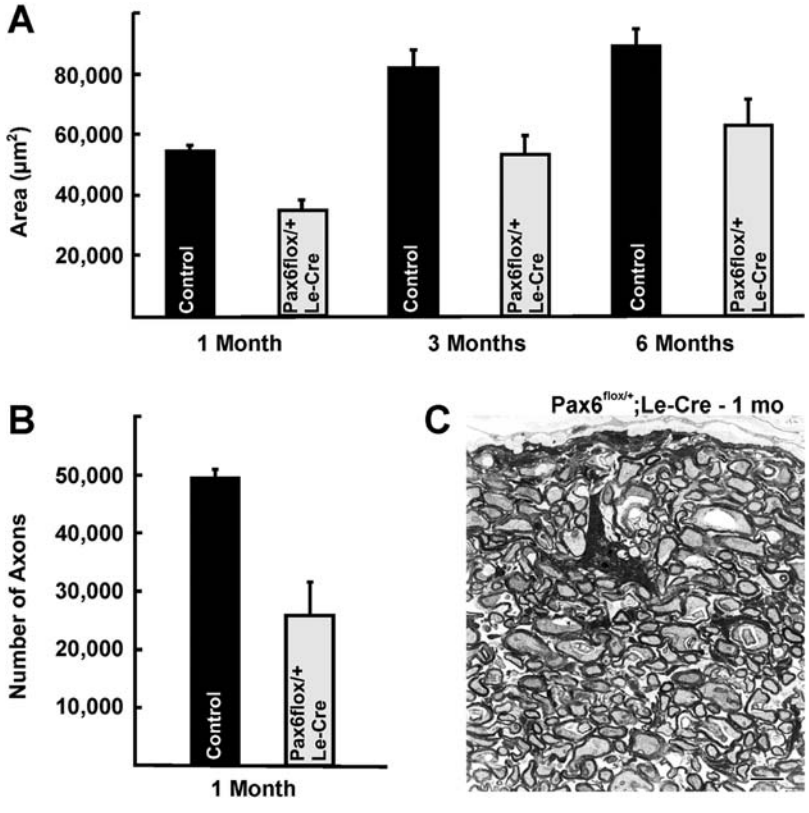

Figure 9. Optic nerves of *Pax6*$^{flox/+}$*;Le-Cre* mice are smaller in area and contain fewer axons than that of control animals. (**A**) Cross-sectional area of optic nerve, mean ± standard deviation (1 month: $n = 2$ for control and experimental each; 3 months: $n = 5$ for control and $n = 4$ for experimental; 6 months; $n = 4$ for control and $n = 5$ for experimental). (**B**) Number of axons in the optic nerve of 1-month-old *Pax6*$^{flox/+}$*;Le-Cre* and control mice ($n = 2$ for control and experimental each). (**C**) Electron micrograph of a cross section through the optic nerve of a 1-month *Pax6*$^{flox/+}$*;Le-Cre* mouse showing myelinated axons and lack of axonal degeneration.

that the increase in IOP in *Pax6*$^{flox/+}$*;Le-Cre* mice causes glaucomatous optic nerve damage.

Aniridia and glaucoma

The exact nature of the developmental defects that cause juvenile glaucoma in humans with *aniridia* is unclear. Grant and Walton (49) performed gonioscopic examinations in aniridic patients with glaucoma versus aniridic patients without glaucoma and found that the stroma of the iris extends forward onto the trabecular meshwork, initially in the form of synechiae-like attachments, followed by a more homogenous sheet, resulting in eventual angle closure. In contrast, the histopathological analysis of the eyes of two children with *aniridia* and Wilm's tumor associated with a partial deletion of the short arm of chromosome 11 (50), where *PAX6* is located (51,52), provided evidence for abnormal trabecular meshwork differentiation and the complete absence of Schlemm's canal. Comparable observations were reported in several earlier histopathological case reports in which the genetic type of *aniridia* had not been determined (53–56). Apparently two mechanisms, a primary developmental effect in the trabecular meshwork outflow pathways, followed by a secondary closure of the iridocorneal angle appear to cause or to contribute to juvenile glaucoma in *aniridia*. This hypothesis is strongly supported by our data obtained in *Pax6*$^{flox/+}$*;Le-Cre* mice, in which the same two mechanisms, failure of trabecular meshwork and Schlemm's canal differentiation, as well as the closure of the iridocorneal angle due to an iridocorneal adhesion of the peripheral iris, were observed. In *Pax6*$^{flox/+}$*;Le-Cre* mice, the structural changes in the iridocorneal angle lead to optic nerve damage and glaucoma and may well do so in humans with *aniridia*. A sequence of events from a primary structural defect in the trabecular meshwork outflow pathways followed by a secondary angle closure may also explain why glaucoma in *aniridia* is not seen after birth, but develops in juvenile age. Uveoscleral outflow which accounts for 25–57% of total aqueous flow in young healthy subjects 20–30 years of age (57–59) may compensate for a while for the loss of function in the trabecular meshwork outflow pathways. The continuous closure of the iridocorneal angle, however, should lead not only to a complete occlusion of the trabecular meshwork outflow pathways, but also minimize access to the uveoscleral outflow route finally leading to a substantial increase in IOP and to glaucoma. Naturally, the extent of the structural phenotype in the iridocorneal angle is likely to vary more in the heterogeneous genetic background of humans than in the more defined genetic background of the mouse strain used for the present study, a fact that may also explain why a substantial percentage of patients with *aniridia* do not develop glaucoma. In addition, there is evidence that the specific type of mutation

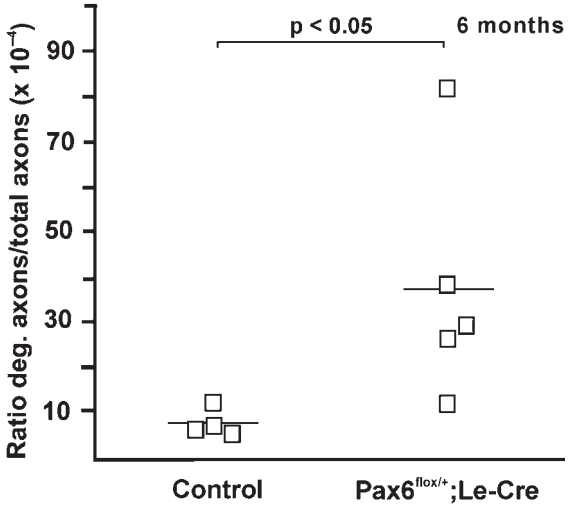

Figure 10. The ratio of degenerating axons versus the total number of axons is higher in optic nerves of 6-month-old *Pax6*$^{flox/+}$*;Le-Cre* mice than in control littermates; $n = 4$ for controls and $n = 5$ for experimental. Horizontal lines represent means. The Student's *t*-test was used for statistical analysis.

in *PAX6* has an effect on the severity of the individual phenotype (60).

Peters' anomaly in *Pax6*$^{flox/+}$*;Le-Cre* mice

In the eyes of newborn *Pax6*$^{flox/+}$;Le-Cre mice, we consistently observed adhesions between the cornea and the lens, and the phenotype of Peters' anomaly corroborating findings from earlier studies in heterozygous Pax6-deficient mice (16,61,62) and *Pax6*$^{flox/+}$*;Le-Cre* mice (24). Similar to our previous finding in the eyes of newborn heterozygous Pax6-deficient mice (16), we detected upon closer examination that the epithelial layers of cornea and lens had not become separated and were in contact through a defect in the central corneal stroma. A comparable phenotype has been observed in mice that are deficient in other transcription factors which contribute to the regulatory processes controlling anterior eye development such as Pitx3, Foxe3, Sip1 and Sox11 (63–69). In heterozygote Pax6-deficient mice, there is evidence that the development of the phenotype of Peters' anomaly is related to a delay in lens placode formation during early eye development (62). We observed in the present study that the lens of young adult *Pax6*$^{flox/+}$*;Le-Cre* mice finally becomes separated from the cornea, whereas only relatively minor defects remain in the central corneal stroma. Obviously, adhesions between cornea and lens are not a permanent scenario in *Pax6*$^{flox/+}$*;Le-Cre* mice. The separation between lens and cornea is delayed, but both tissues finally disconnect when the development of the anterior eye is complete. Adhesions between cornea and lens and a persisting lens stalk are not commonly seen in patients with *aniridia* (6,7), although some cases with mutations in PAX6 and Peters' anomaly have been reported (70).

Molecular signals from the lens control the development of the iridocorneal angle

Although *Pax6*$^{flox/+}$*;Le-Cre* mice show a selective reduction in Pax6 expression in epithelial cells of the lens and the cornea, as well as in amacrine cells, it appears most likely that it is the reduced amount of Pax6 in lens cells, which is causative for the structural changes in the development of the iridocorneal angle. For example, Pax6 might control the transcription of genes encoding signaling molecules in lens cells that are required to control the sequence of the molecular events that occur during the development of the iridocorneal angle. Such molecules might be secreted from lens cells into the aqueous humor to reach target cells in the iridocorneal angle. In a recent study, Wolf *et al*. (71) used DNA microarrays to identify genes that are expressed differentially between 1-day-old mouse Pax6 heterozygous and wild-type lenses. Among the genes that were indentified as down-regulated in heterozygous Pax6-deficient mice was that encoding for transforming growth factor-β2 (TGF-β2). Additional experiments showed that the locus encoding TGF-β2, which was positively regulated by Pax6, was occupied by Pax6 in lens chromatin. In addition, using *in vitro* assays, at least three Pax6-binding sites were identified in the TGF-β2 promoter region. Overall, the findings strongly indicate that the transcription of TGF-β2 is under the direct control of Pax6. TGF-β2 is a member of a family of dimeric polypeptide growth factors. In the aqueous humor of the normal eye, TGF-β2, which is secreted from the epithelial cells of ciliary body (72) and lens (73–75), is found at relative high concentrations (76–78). The physiological role of TGF-β2 in the aqueous humor appears to be tightly linked with the immunosuppressive environment of the anterior chamber (79,80) and the phenomenon of anterior chamber-associated immune deviation. In addition, there is substantial evidence that TGF-β2 regulates the turnover of extracellular matrix in the trabecular meshwork (81). It is not unlikely that the action of TGF-β2 on extracellular matrix turnover in the trabecular meshwork is required during differentiation of the iridocorneal angle and that reduced amounts of TGF-β2 in the aqueous humor, caused by the reduction of Pax6 in lens cells, result in the failure of iridocorneal angle development both in *Pax6*$^{flox/+}$*;Le-Cre* mice and in human patients with *aniridia*. In support of this hypothesis are recent findings by Iwao *et al*. (82) who reported that mice which are deficient in heparan sulfate show disruption of TGF-β2 signaling, an effect that correlates with Peters' anomaly, anterior chamber dysgenesis and developmental glaucoma. An adhesion of the lens to the cornea and the phenotype of Peters' anomaly has been observed in TGF-β2-deficient mice (83), quite similar to that observed in *Pax6*$^{flox/+}$*;Le-Cre* mice. TGF-β2-deficient mice die at birth because of cardiac defects (84), and several days before the development of the iridocorneal angle is complete in the mouse eye (9). Although the available data strongly indicate that TGF-β2 secreted from the lens is the key signaling molecule to control the morphogenetic events during the development of the iridocorneal angle, different mouse lines need to be developed to finally clarify this question, and such experiments are currently underway in our laboratory.

MATERIALS AND METHODS

Mouse lines

Pax6$^{flox/flox}$, Le-Cre, α-Cre and *Pax6*$^{-/+}$ mice were established as described (16,31,85). Pax6$^{flox/+}$; Pax6$^{flox/+}$;Le-Cre and

littermate controls ($Pax6^{flox/+}$ or $Pax6^{+/+}$;Le-Cre) were obtained by crossing $Pax6^{flox/+}$ with Le-Cre mice. $Pax6^{flox/+}$;$Pax6^{flox/+}$;α-Cre and littermate controls ($Pax6^{flox/+}$ or $Pax6^{+/+}$;α-Cre) were obtained by crossing $Pax6^{flox/+}$ with α-Cre mice. The day of birth was referred to as P1. Analyses were conducted on F1 progeny from a mating between ICR and FVB/NJ genetic backgrounds. $Pax6^{-/+}$ mice were kept in an NMRI background.

Light and electron microscopy

Eyes were obtained from newborn mice every day between P1 and P14 and from animals at 3 weeks and 1, 3 and 6 months of age. Eyes were enucleated, fixed in Karnovsky's solution (2.5% glutaraldehyde and 2.5% paraformaldehyde in 0.1 M cacodylate buffer) for 24 h (86). After rinsing in 0.1 M cacodylate buffer, post-fixation was accomplished in a mixture of 1% OsO_4 and 0.8% potassium ferrocyanide in 0.1 M cacodylate buffer for 2 h at 4°C. Eyes were then dehydrated in a graded series of ethanol and embedded in Epon (Serva, Heidelberg, Germany). Semithin sections (1 μm) were collected on uncoated glass slides and stained with methylene blue/azure II (87). Ultrathin sections were mounted on uncoated copper grids, stained with uranyl acetate and lead citrate and examined on a Zeiss EM 10 A electron microscope. Myelinated optic nerve axons were visualized by PPD (Roth) staining of Epon-embedded semithin sections (88). In brief, 1% PPD in 98% ethanol was freshly prepared and stored at daylight for 3 days prior to use until the solution had darkened. The solution is stable for 1 week in the dark at 4°C. Optic nerve cross sections were stained for 2–3 min at room temperature and staining was differentiated with changes of 100% ethanol. To count the number of optic nerve axons in 3- and 6-month-old animals, PPD stained cross sections were visualized by bright field microscopy using a ×100 oil immersion objective for highest resolution. In 1-month-old animals, in which the myelin sheath of optic nerve axons is still thin, electron micrographs of the entire cross-sectioned optic nerve area were mounted and analyzed. Myelinated axons were identified and counted software assisted (Axiovision software 3.0 Carl Zeiss, Jena, Germany).

Measurement of IOP

IOP was measured invasively in the eyes of 10-week-old $Pax6^{flox/+}$;Le-Cre mice (body weight 27–30 g) and wild-type littermates as described previously (89,90). Measurements were performed at the same time of day. The animals were deeply anaesthetized by intramuscular injection of a mixture of ketamine as hydrochloride (100 mg/kg, Parke-Davis, Freiburg, Germany) and xylazine (5 mg/kg, Bayer Leverkusen, Leverkusen, Germany) and placed on a surgical platform. The eye was viewed under a dissecting microscope, and the microneedle (size 30 G) tip was placed inside a drop of PBS on the top of the eye. At this point, the pressure reading was zeroed. The tip of the microneedle was manually inserted into the anterior chamber with the IOP recorded continuously. The IOP values usually reached a plateau after 1 s of higher IOP values due to the needle insertion. If the plateau was constant for 1 min, the eye was given some gentle extra pressure from outside to confirm microneedle patency. This manipulation resulted in some IOP peaks that returned to the prior plateau level. The microneedle was then withdrawn from the anterior chamber; rapid return of the pressure to zero was required for the inclusion of data. The original measurements were calibrated in cmH_2O. For statistical analysis, a Student's *t*-test was performed.

IOP was measured non-invasively in eyes of sedated mice (100 mg/kg ketamine and 10 mg/kg xylazine injected i.p.). Measurements were conducted at the same time of day using the TonoLab tonometer (Tiolat, Helsinki, Finland). Each reading was comprised of six measurements averaged automatically. Highly and moderately variable readings were excluded. An average of five readings was considered as a single result; presented values are the average of 10 eyes per genotype at each time point (same mice at different ages). Statistical analysis was performed by the two-way ANOVA. Comparable data were obtained from additional litters, but were excluded from the study due to an incomplete analysis.

ACKNOWLEDGEMENTS

The technical help of Margit Schimmel is greatly appreciated.

Conflict of Interest statement. None declared.

FUNDING

This work was supported by the Deutsche Forschungsgemeinschaft (FOR 1075, TP5 to E.R.T.), the German-Israeli-Foundation (I-756-187.2/2002 to E.R.T. and R.A.-P.) and the Glaucoma Research Foundation (pilot project grant to R.A.-P.).

REFERENCES

1. Gehring, W.J. (2002) The genetic control of eye development and its implications for the evolution of the various eye-types. *Int. J. Dev. Biol.*, **46**, 65–73.
2. Ashery-Padan, R. and Gruss, P. (2001) Pax6 lights-up the way for eye development. *Curr. Opin. Cell Biol.*, **13**, 706–714.
3. Chow, R.L. and Lang, R.A. (2001) Early eye development in vertebrates. *Annu. Rev. Cell Dev. Biol.*, **17**, 255–296.
4. Kozmik, Z. (2008) The role of Pax genes in eye evolution. *Brain Res. Bull.*, **75**, 335–339.
5. Mintz-Hittner, H.A. (1996) Aniridia. In Ritch, R., Shields, M.B. and Krupin, T. (eds), *The Glaucomas*. Mosby, St Louis, pp. 859–874.
6. Brauner, S.C., Walton, D.S. and Chen, T.C. (2008) Aniridia. *Int. Ophthalmol. Clin.*, **48**, 79–85.
7. Lee, H., Khan, R. and O'Keefe, M. (2008) Aniridia: current pathology and management. *Acta Ophthalmol. (Copenh.)*, **86**, 708–715.
8. Prosser, J. and van Heyningen, V. (1998) PAX6 mutations reviewed. *Hum. Mutat.*, **11**, 93–108.
9. Cvekl, A. and Tamm, E.R. (2004) Anterior eye development and ocular mesenchyme: new insights from mouse models and human diseases. *Bioessays*, **26**, 374–386.
10. Hogan, B.L., Hirst, E.M., Horsburgh, G. and Hetherington, C.M. (1988) Small eye (Sey): a mouse model for the genetic analysis of craniofacial abnormalities. *Development*, **103** (suppl.), 115–119.
11. Glaser, T., Lane, J. and Housman, D. (1990) A mouse model of the aniridia-Wilms tumor deletion syndrome. *Science*, **250**, 823–827.
12. Theiler, K. and Varnum, D.S. (1981) Development of coloboma (Cm/+), a mutation with anterior lens adhesion. *Anat. Embryol. (Berl.)*, **162**, 121–126.

13. Theiler, K., Varnum, D.S. and Stevens, L.C. (1978) Development of Dickie's small eye, a mutation in the house mouse. *Anat. Embryol. (Berl.)*, **155**, 81–86.
14. Johnson, M. (2006) What controls aqueous humour outflow resistance?. *Exp. Eye Res.*, **82**, 545–557.
15. Tamm, E.R. (2009) The trabecular meshwork outflow pathways: structural and functional aspects. *Exp. Eye Res.*, **88**, 648–655.
16. Baulmann, D., Ohlmann, A., Flügel-Koch, C., Goswami, S., Cvekl, A. and Tamm, E.R. (2002) *Pax6* heterozygous eyes show defects in chamber angle differentiation that are associated with a wide spectrum of other anterior eye segment abnormalities. *Mech. Dev.*, **118**, 3–17.
17. Grindley, J.C., Davidson, D.R. and Hill, R.E. (1995) The role of *pax-6* in eye and nasal development. *Development*, **121**, 1433–1442.
18. Walther, C. and Gruss, P. (1991) Pax-6, a murine paired box gene, is expressed in the developing CNS. *Development*, **113**, 1435–1449.
19. Koroma, B.M., Yang, J.M. and Sundin, O.H. (1997) The Pax-6 homeobox gene is expressed throughout the corneal and conjunctival epithelia. *Invest. Ophthalmol. Vis. Sci.*, **38**, 108–120.
20. Nishina, S., Kohsaka, S., Yamaguchi, Y., Handa, H., Kawakami, A., Fujisawa, H. and Azuma, N. (1999) PAX6 expression in the developing human eye. *Br. J. Ophthalmol.*, **83**, 723–727.
21. Tamm, E.R. (2004) Genetic changes and their influence on structure and function of the eye in glaucoma. In Grehn, F.J. and Stamper, R. (eds), *Essentials in Opthalmology. Glaucoma*. Springer, Berlin, Heidelberg, NY.
22. Ramaesh, T., Collinson, J.M., Ramaesh, K., Kaufman, M.H., West, J.D. and Dhillon, B. (2003) Corneal abnormalities in Pax6+/− small eye mice mimic human aniridia-related keratopathy. *Invest. Ophthalmol. Vis. Sci.*, **44**, 1871–1878.
23. Kanakubo, S., Nomura, T., Yamamura, K., Miyazaki, J., Tamai, M. and Osumi, N. (2006) Abnormal migration and distribution of neural crest cells in Pax6 heterozygous mutant eye, a model for human eye diseases. *Genes Cells*, **11**, 919–933.
24. Davis-Silberman, N., Kalich, T., Oron-Karni, V., Marquardt, T., Kroeber, M., Tamm, E.R. and Ashery-Padan, R. (2005) Genetic dissection of Pax6 dosage requirements in the developing mouse eye. *Hum. Mol. Genet.*, **14**, 2265–2276.
25. Kammandel, B., Chowdhury, K., Stoykova, A., Aparicio, S., Brenner, S. and Gruss, P. (1999) Distinct cis-essential modules direct the time-space pattern of the Pax6 gene activity. *Dev. Biol.*, **205**, 79–97.
26. Griffin, C., Kleinjan, D.A., Doe, B. and van Heyningen, V. (2002) New 3′ elements control Pax6 expression in the developing pretectum, neural retina and olfactory region. *Mech. Dev.*, **112**, 89–100.
27. Kleinjan, D.A., Seawright, A., Mella, S., Carr, C.B., Tyas, D.A., Simpson, T.I., Mason, J.O., Price, D.J. and van Heyningen, V. (2006) Long-range downstream enhancers are essential for Pax6 expression. *Dev. Biol.*, **299**, 563–581.
28. Morgan, R. (2004) Conservation of sequence and function in the Pax6 regulatory elements. *Trends Genet.*, **20**, 283–287.
29. Dimanlig, P.V., Faber, S.C., Auerbach, W., Makarenkova, H.P. and Lang, R.A. (2001) The upstream ectoderm enhancer in Pax6 has an important role in lens induction. *Development*, **128**, 4415–4424.
30. Ethier, C.R. (2002) The inner wall of Schlemm's canal. *Exp. Eye Res.*, **74**, 161–172.
31. Marquardt, T., Ashery-Padan, R., Andrejewski, N., Scardigli, R., Guillemot, F. and Gruss, P. (2001) Pax6 is required for the multipotent state of retinal progenitor cells. *Cell*, **105**, 43–55.
32. Do, C.W. and Civan, M.M. (2009) Species variation in biology and physiology of the ciliary epithelium: similarities and differences. *Exp. Eye Res.*, **88**, 631–640.
33. Overby, D.R., Stamer, W.D. and Johnson, M. (2009) The changing paradigm of outflow resistance generation: towards synergistic models of the JCT and inner wall endothelium. *Exp. Eye Res.*, **88**, 656–670.
34. Alm, A. and Nilsson, S.F. (2009) Uveoscleral outflow—a review. *Exp. Eye Res.*, **88**, 760–768.
35. Tamm, E.R. and Kellenberger, A. (2008) Aqueous humor dynamics and trabecular meshwork. In Chalupa, L.M. and Williams, R.W. (eds), *Eye, Retina, and Visual System of the Mouse*. MIT Press, Cambridge, pp. 129–134.
36. Aihara, M., Lindsey, J.D. and Weinreb, R.N. (2003) Aqueous humor dynamics in mice. *Invest. Ophthalmol. Vis. Sci.*, **44**, 5168–5173.
37. The AGIS Investigators. (2000) The advanced glaucoma intervention study (AGIS): 7. The relationship between control of intraocular pressure and visual field deterioration. *Am. J. Ophthalmol.*, **130**, 429–440.
38. Collaborative Normal-Tension Glaucoma Study Group. (1998) The effectiveness of intraocular pressure reduction in the treatment of normal-tension glaucoma. Collaborative Normal-Tension Glaucoma Study Group. *Am. J. Ophthalmol.*, **126**, 498–505.
39. Leske, M.C., Heijl, A., Hussein, M., Bengtsson, B., Hyman, L. and Komaroff, E. (2003) Factors for glaucoma progression and the effect of treatment: the early manifest glaucoma trial. *Arch. Ophthalmol.*, **121**, 48–56.
40. Collaborative Normal-Tension Glaucoma Study Group. (1998) Comparison of glaucomatous progression between untreated patients with normal-tension glaucoma and patients with therapeutically reduced intraocular pressures. *Am. J. Ophthalmol.*, **126**, 487–497.
41. Higginbotham, E.J., Gordon, M.O., Beiser, J.A., Drake, M.V., Bennett, G.R., Wilson, M.R. and Kass, M.A. (2004) The Ocular Hypertension Treatment Study: topical medication delays or prevents primary open-angle glaucoma in African American individuals. *Arch. Ophthalmol.*, **122**, 813–820.
42. Gordon, M.O., Beiser, J.A., Brandt, J.D., Heuer, D.K., Higginbotham, E.J., Johnson, C.A., Keltner, J.L., Miller, J.P., Parrish, R.K. 2nd, Wilson, M.R. *et al.* (2002) The Ocular Hypertension Treatment Study: baseline factors that predict the onset of primary open-angle glaucoma. *Arch. Ophthalmol.*, **120**, 714–720; discussion 829–730.
43. Anderson, M.G., Smith, R.S., Hawes, N.L., Zabaleta, A., Chang, B., Wiggs, J.L. and John, S.W. (2002) Mutations in genes encoding melanosomal proteins cause pigmentary glaucoma in DBA/2J mice. *Nat. Genet.*, **30**, 81–85.
44. Senatorov, V., Malyukova, I., Fariss, R., Wawrousek, E.F., Swaminathan, S., Sharan, S.K. and Tomarev, S. (2006) Expression of mutated mouse myocilin induces open-angle glaucoma in transgenic mice. *J. Neurosci.*, **26**, 11903–11914.
45. Howell, G.R., Libby, R.T. and John, S.W. (2008) Mouse genetic models: an ideal system for understanding glaucomatous neurodegeneration and neuroprotection. *Prog. Brain Res.*, **173**, 303–321.
46. Gould, D.B., Marchant, J.K., Savinova, O.V., Smith, R.S. and John, S.W. (2007) Col4a1 mutation causes endoplasmic reticulum stress and genetically modifiable ocular dysgenesis. *Hum. Mol. Genet.*, **16**, 798–807.
47. Dangata, Y.Y., Findlater, G.S., Dhillon, B. and Kaufman, M.H. (1994) Morphometric study of the optic nerve of adult normal mice and mice heterozygous for the small eye mutation (Sey/+). *J. Anat.*, **185** (Pt 3), 627–635.
48. Howell, G.R., Libby, R.T., Jakobs, T.C., Smith, R.S., Phalan, F.C., Barter, J.W., Barbay, J.M., Marchant, J.K., Mahesh, N., Porciatti, V. *et al.* (2007) Axons of retinal ganglion cells are insulted in the optic nerve early in DBA/2J glaucoma. *J. Cell Biol.*, **179**, 1523–1537.
49. Grant, W.M. and Walton, D.S. (1974) Progressive changes in the angle in congenital aniridia, with development of glaucoma. *Am. J. Ophthalmol.*, **78**, 842–847.
50. Margo, C.E. (1983) Congenital aniridia: a histopathologic study of the anterior segment in children. *J. Pediatr. Ophthalmol. Strabismus*, **20**, 192–198.
51. Ton, C.C., Miwa, H. and Saunders, G.F. (1992) Small eye (Sey): cloning and characterization of the murine homolog of the human aniridia gene. *Genomics*, **13**, 251–256.
52. Jordan, T., Hanson, I., Zaletayev, D., Hodgson, S., Prosser, J., Seawright, A., Hastie, N. and van Heyningen, V. (1992) The human PAX6 gene is mutated in two patients with aniridia. *Nat. Genet.*, **1**, 328–332.
53. Collins, T. (1893) Congenital defects of the iris and glaucoma. *Trans. Ophthalmol. Soc. UK*, **13**, 128–139.
54. Bergmeister, R. (1904) Zwei Fälle von angeborener Irideremie. *Graefes Arch. Clin. Exp. Ophthalmol.*, **59**, 31–45.
55. Callahan, A. (1949) Aniridia with ectopia lentis and secondary glaucoma. *Am. J. Ophthalmol.*, **32**, 28–40.
56. Duke-Elder, S. (1964) Hypoplasia of the iris: aniridia. In Duke-Elder, S. (ed.), *System of Ophthalmology. Vol. III. Normal and Abnormal Development. Part 2: Congenital Disorders*. Henry Kimpton, London, pp. 565–572.
57. Townsend, D.J. and Brubaker, R.F. (1980) Immediate effect of epinephrine on aqueous formation in the normal eye as measured by fluorophotometry. *Invest. Ophthalmol. Vis. Sci.*, **196**, 256–266.
58. Mishima, H.K., Kiuchi, Y., Takamatsu, M., Racz, P. and Bito, L.Z. (1997) Circadian intraocular pressure management with latanoprost: diurnal and nocturnal intraocular pressure reduction and increased uveoscleral outflow. *Surv. Ophthalmol.*, **41** (Suppl. 2), S139–S144.

59. Toris, C.B., Camras, C.B. and Yablonski, M.E. (1999) Acute versus chronic effects of brimonidine on aqueous humor dynamics in ocular hypertensive patients. *Am. J. Ophthalmol.*, **128**, 8–14.
60. Hingorani, M., Williamson, K.A., Moore, A.T. and van Heyningen, V. (2009) Detailed ophthalmologic evaluation of 43 individuals with PAX6 mutations. *Invest. Ophthalmol. Vis. Sci.*, **50**, 2581–2590.
61. Collinson, J.M., Quinn, J.C., Buchanan, M.A., Kaufman, M.H., Wedden, S.E., West, J.D. and Hill, R.E. (2001) Primary defects in the lens underlie complex anterior segment abnormalities of the Pax6 heterozygous eye. *Proc. Natl Acad. Sci. USA*, **98**, 9688–9693.
62. van Raamsdonk, C.D. and Tilghman, S.M. (2000) Dosage requirement and allelic expression of PAX6 during lens placode formation. *Development*, **127**, 5439–5448.
63. Semina, E.V., Murray, J.C., Reiter, R., Hrstka, R.F. and Graw, J. (2000) Deletion in the promoter region and altered expression of Pitx3 homeobox gene in aphakia mice. *Hum. Mol. Genet.*, **9**, 1575–1585.
64. Rieger, D.K., Reichenberger, E., McLean, W., Sidow, A. and Olsen, B.R. (2001) A double-deletion mutation in the Pitx3 gene causes arrested lens development in aphakia mice. *Genomics*, **72**, 61–72.
65. Varnum, D.S. and Stevens, L.C. (1968) Aphakia, a new mutation in the mouse. *J. Hered.*, **59**, 147–150.
66. Medina-Martinez, O., Brownell, I., Amaya-Manzanares, F., Hu, Q., Behringer, R.R. and Jamrich, M. (2005) Severe defects in proliferation and differentiation of lens cells in Foxe3 null mice. *Mol. Cell Biol.*, **25**, 8854–8863.
67. Blixt, A., Landgren, H., Johansson, B.R. and Carlsson, P. (2007) Foxe3 is required for morphogenesis and differentiation of the anterior segment of the eye and is sensitive to Pax6 gene dosage. *Dev. Biol.*, **302**, 218–229.
68. Yoshimoto, A., Saigou, Y., Higashi, Y. and Kondoh, H. (2005) Regulation of ocular lens development by Smad-interacting protein 1 involving Foxe3 activation. *Development*, **132**, 4437–4448.
69. Wurm, A., Sock, E., Fuchshofer, R., Wegner, M. and Tamm, E.R. (2008) Anterior segment dysgenesis in the eyes of mice deficient for the high-mobility-group transcription factor Sox11. *Exp. Eye Res.*, **86**, 895–907.
70. Hanson, I.M., Fletcher, J.M., Jordan, T., Brown, A., Taylor, D., Adams, R.J., Punnett, H.H. and van, H.V. (1994) Mutations at the PAX6 locus are found in heterogeneous anterior segment malformations including Peters' anomaly. *Nat. Genet.*, **6**, 168–173.
71. Wolf, L.V., Yang, Y., Wang, J., Xie, Q., Braunger, B., Tamm, E.R., Zavadil, J. and Cvekl, A. (2009) Identification of pax6-dependent gene regulatory networks in the mouse lens. *PLoS One*, **4**, e4159.
72. Helbig, H., Kittredge, K.L., Coca-Prados, M., Davis, J., Palestine, A.G. and Nussenblatt, R.B. (1991) Mammalian ciliary-body epithelial cells in culture produce transforming growth factor-beta. *Graefes Arch. Clin. Exp. Ophthalmol.*, **229**, 84–87.
73. Allen, J.B., Davidson, M.G., Nasisse, M.P., Fleisher, L.N. and McGahan, M.C. (1998) The lens influences aqueous humor levels of transforming growth factor-beta 2. *Graefes Arch. Clin. Exp. Ophthalmol.*, **236**, 305–311.
74. Gordon-Thomson, C., de Iongh, R.U., Hales, A.M., Chamberlain, C.G. and McAvoy, J.W. (1998) Differential cataractogenic potency of TGF-beta1, -beta2 and -beta3 and their expression in the postnatal rat eye. *Invest. Ophthalmol. Vis. Sci.*, **39**, 1399–1409.
75. Wallentin, N., Wickstrom, K. and Lundberg, C. (1998) Effect of cataract surgery on aqueous TGF-beta and lens epithelial cell proliferation. *Invest. Ophthalmol. Vis. Sci.*, **39**, 1410–1418.
76. Granstein, R.D., Staszewski, R., Knisley, T.L., Zeira, E., Nazareno, R., Latina, M. and Albert, D.M. (1990) Aqueous humor contains transforming growth factor-β and a small (<3500 Daltons) inhibitor of thymocyte proliferation. *J. Immunol.*, **144**, 3021–3027.
77. Jampel, H.D., Roche, N., Stark, W.J. and Roberts, A.B. (1990) Transforming growth factor-β in human aqueous humor. *Curr. Eye Res.*, **9**, 963–969.
78. Cousins, S.W., McCabe, M.M., Danielpour, D. and Streilein, J.W. (1991) Identification of transforming growth factor-beta as an immunosuppressive factor in aqueous humor. *Invest. Ophthalmol. Vis. Sci.*, **32**, 2201–2211.
79. Streilein, J.W., Ksander, B.R. and Taylor, A.W. (1997) Immune deviation in relation to ocular immune privilege. *J. Immunol.*, **158**, 3557–3560.
80. Streilein, J.W. (1999) Immunoregulatory mechanisms of the eye. *Prog. Retin. Eye Res.*, **18**, 357–370.
81. Fuchshofer, R. and Tamm, E.R. (2009) Modulation of extracellular matrix turnover in the trabecular meshwork. *Exp. Eye Res.*, **88**, 683–688.
82. Iwao, K., Inatani, M., Matsumoto, Y., Ogata-Iwao, M., Takihara, Y., Irie, F., Yamaguchi, Y., Okinami, S. and Tanihara, H. (2009) Heparan sulfate deficiency leads to Peters anomaly in mice by disturbing neural crest TGF-beta2 signaling. *J. Clin. Invest.*, **119**, 1997–2008.
83. Saika, S., Liu, C.Y., Azhar, M., Sanford, L.P., Doetschman, T., Gendron, R.L., Kao, C.W. and Kao, W.W. (2001) TGFbeta2 in corneal morphogenesis during mouse embryonic development. *Dev. Biol.*, **240**, 419–432.
84. Sanford, L.P., Ormsby, I., Gittenberger-de Groot, A.C., Sariola, H., Friedman, R., Boivin, G.P., Cardell, E.L. and Doetschman, T. (1997) TGFbeta2 knockout mice have multiple developmental defects that are non- overlapping with other TGFbeta knockout phenotypes. *Development*, **124**, 2659–2670.
85. Ashery-Padan, R., Marquardt, T., Zhou, X. and Gruss, P. (2000) Pax6 activity in the lens primordium is required for lens formation and for correct placement of a single retina in the eye. *Genes Dev.*, **14**, 2701–2711.
86. Karnovsky, M.J. (1965) A formaldehyde-glutaraldehyde fixative of high osmolality for use in electron-microscopy. *J. Cell Biol.*, **27**, 137–138.
87. Richardson, K.C., Jarret, L. and Finke, H. (1960) Embedding in epoxy resins for ultrathin sectioning in electron microscopy. *Stain Technol.*, **35**, 313–323.
88. Schultze, W.H. (1972) Über das Paraphenylendiamin in der histologischen Färbetechnik und über eine neue Schnellfärbemethode der Nervenmarkscheide am Gefrierschnitt. *Zentralbl. Pathol.*, **36**, 639–640.
89. John, S.W., Hagaman, J.R., MacTaggart, T.E., Peng, L. and Smithes, O. (1997) Intraocular pressure in inbred mouse strains. *Invest. Ophthalmol. Vis. Sci.*, **38**, 249–253.
90. Zillig, M., Wurm, A., Grehn, F.J., Russell, P. and Tamm, E.R. (2005) Overexpression and properties of wild-type and Tyr437His mutated myocilin in the eyes of transgenic mice. *Invest. Ophthalmol. Vis. Sci.*, **46**, 223–234.